

Supplementary data for the article:

Korać, J.; Stanković, D. M.; Stanić, M.; Bajuk-Bogdanović, D.; Žižić, M.; Pristov, J. B.; Grgurić-Šipka, S.; Popović-Bijelić, A.; Spasojević, I. Coordinate and Redox Interactions of Epinephrine with Ferric and Ferrous Iron at Physiological PH. *Scientific Reports* **2018**, *8* (1). <https://doi.org/10.1038/s41598-018-21940-7>

**Coordinate and redox interactions of epinephrine with ferric and ferrous iron at
physiological pH**

Jelena Korać, Dalibor M. Stanković, Marina Stanić, Danica Bajuk-Bogdanović, Milan Žižić,
Jelena Bogdanović Pristov, Sanja Grgurić-Šipka, Ana Popović-Bijelić, Ivan Spasojević

Supplementary Information

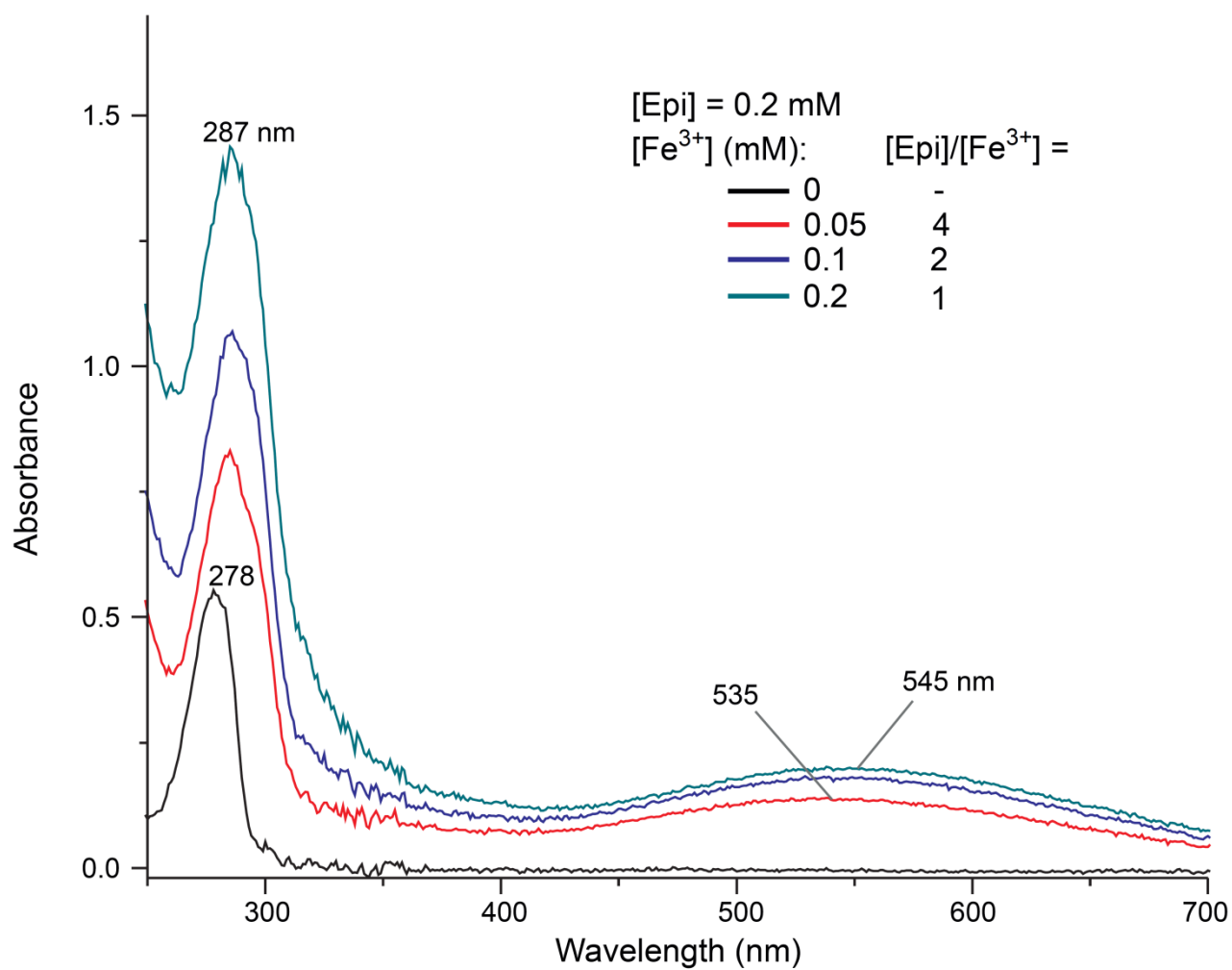


Figure S1 UV/Vis spectra of Epi and ferric iron in 10 mM phosphate buffer, pH 7.4. In contrast to Tris, the same complex appears to predominate at both low and high [Epi]/[Fe³⁺] ($\lambda_{\text{max}} = 545 \text{ nm}$), most likely in relation to the high affinity of phosphates for Fe³⁺. The spectra were acquired following 15 min incubation, and remained unaltered for at least 1 h.

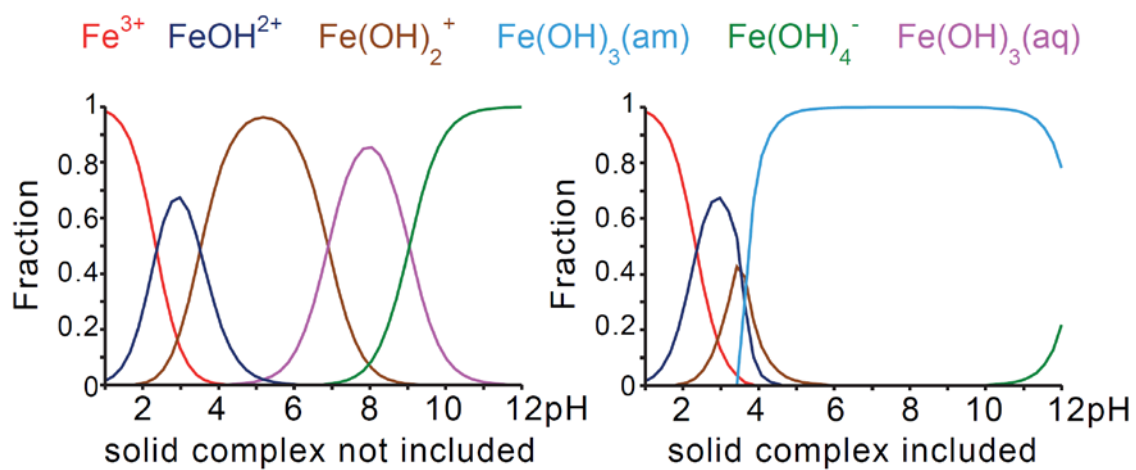


Figure S2 Speciation diagrams of Fe^{3+} in water. Diagrams were prepared in Hydra-Medusa Software, using the following parameters: $[\text{Fe}^{3+}] = 0.1 \text{ mM}$; pH range 1–12; $T = 293 \text{ K}$.

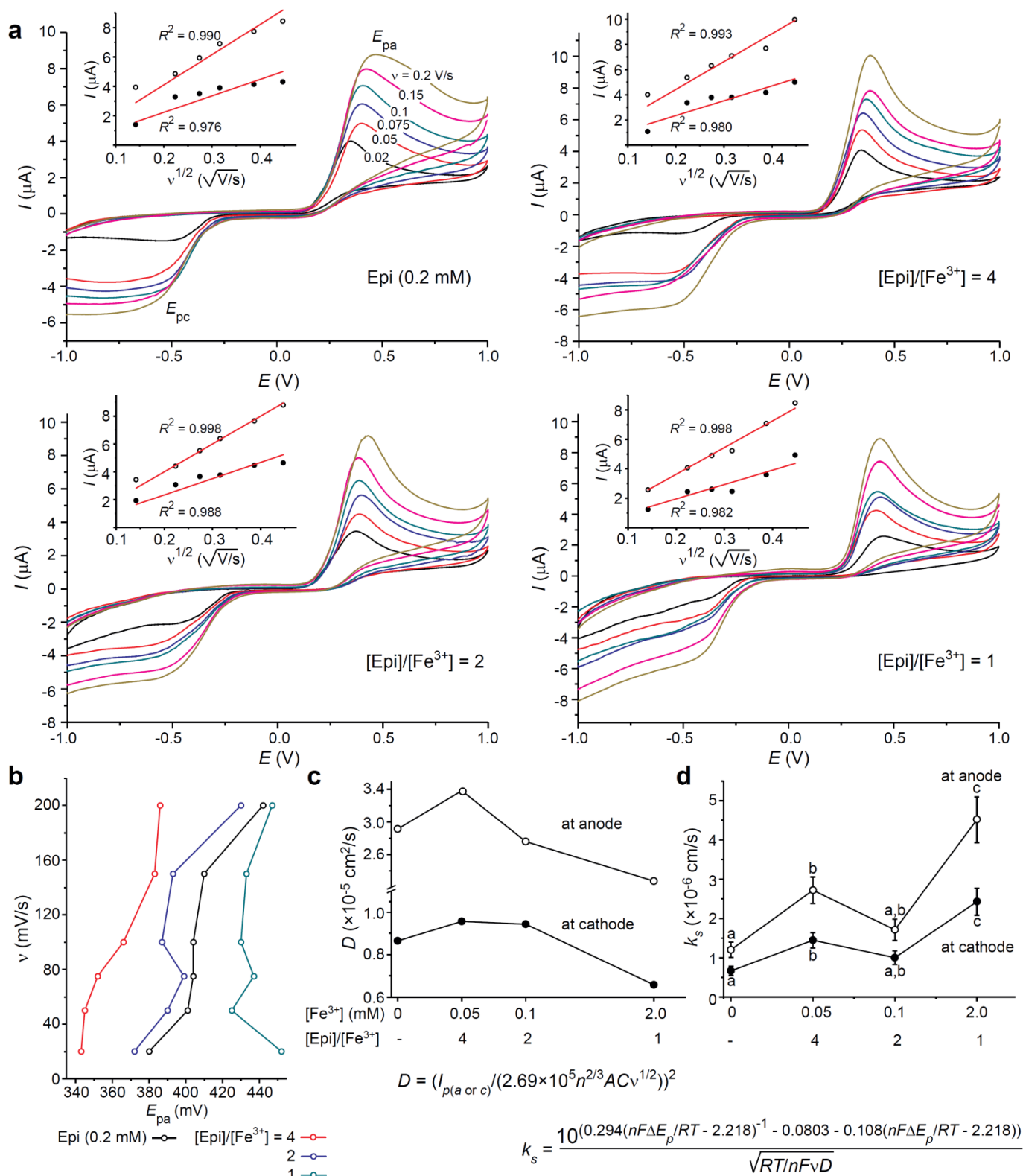


Figure S3 Scan rate analysis of the Epi/Fe³⁺ systems. (a) Cyclic voltammograms of Epi in absence or presence of Fe³⁺ at the boron doped diamond electrode obtained at different scan rates ($v = 0.02\text{--}0.2$ V/s). The inset figures in each panel represent the dependence between I_{pa} (open circles) and I_{pc} (closed circles; absolute values) and $v^{1/2}$. Linear fit and R^2 values are presented. (b) E_{pa} for Epi and $[Epi]/[Fe^{3+}] = 4, 2, 1$.

and 1 at different v . (c) D for Epi and different $[\text{Epi}]/[\text{Fe}^{3+}]$. Randles–Sevcik equation (at the bottom middle): n , number of transferred e^- ; A , area of the working electrode (0.0707 cm^2); C , concentration of redox species in solution (mol/cm^3). (d) Rate constants of electron transfer (k_s) for Epi and different $[\text{Epi}]/[\text{Fe}^{3+}]$. Results are presented as means (\pm SE) of measurements made at various v . k_s not sharing a common letter are significantly different ($P < 0.05$). Nicholson Shain calculus (at the bottom right): R , standard gas constant; T , temperature (298 K); F , Faraday's constant; ΔE_p , the difference between E_{pa} and E_{pc} taken at various v .

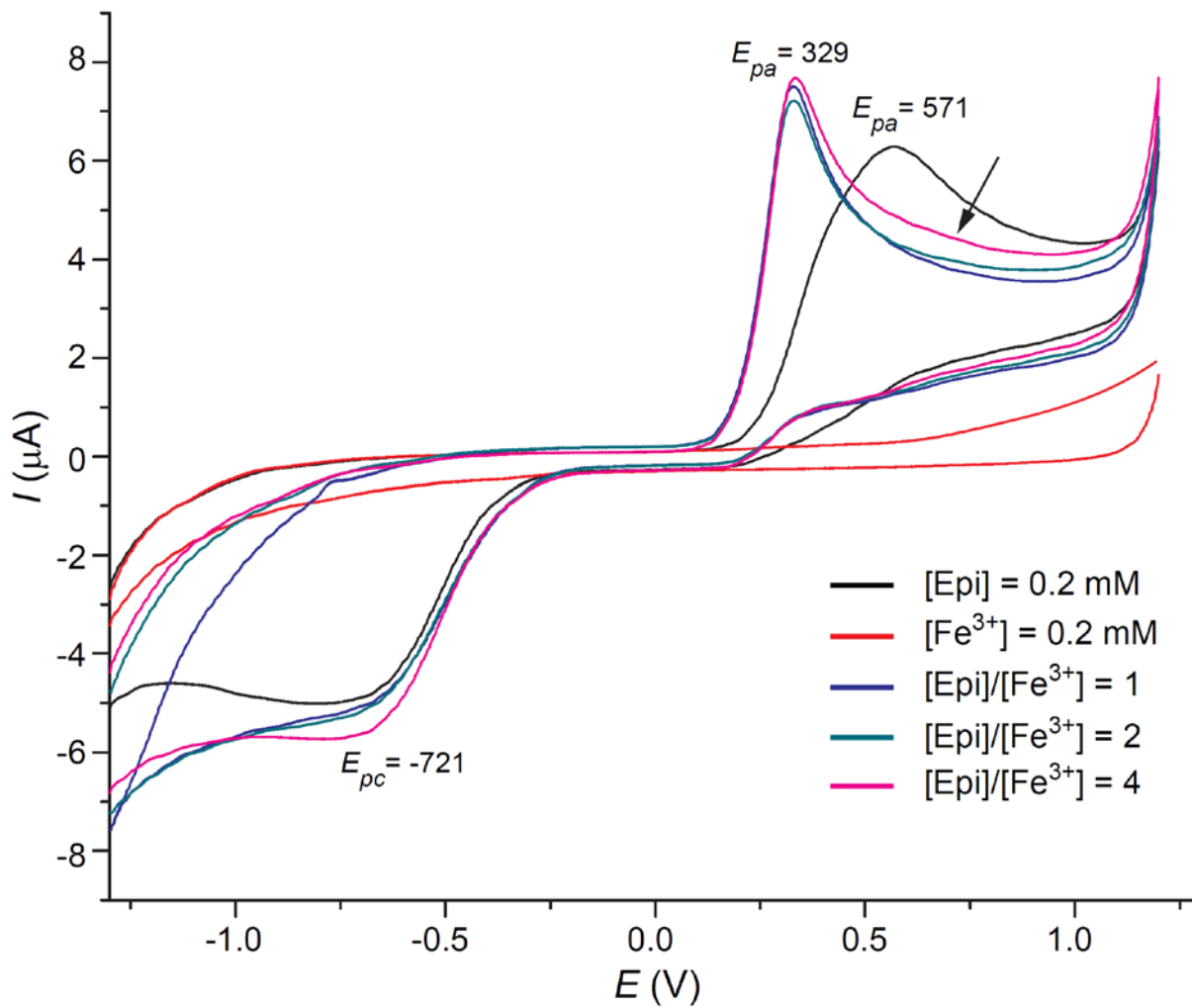


Figure S4 Cyclic voltammograms of Epi in absence or presence of Fe^{3+} in 10 mM potassium phosphate buffer, pH 7.4, at the boron doped diamond electrode. The oxidation/anodic (E_{pa}) and reduction/cathodic (E_{pc}) potentials are presented. Scan rate was 0.1 V/s.

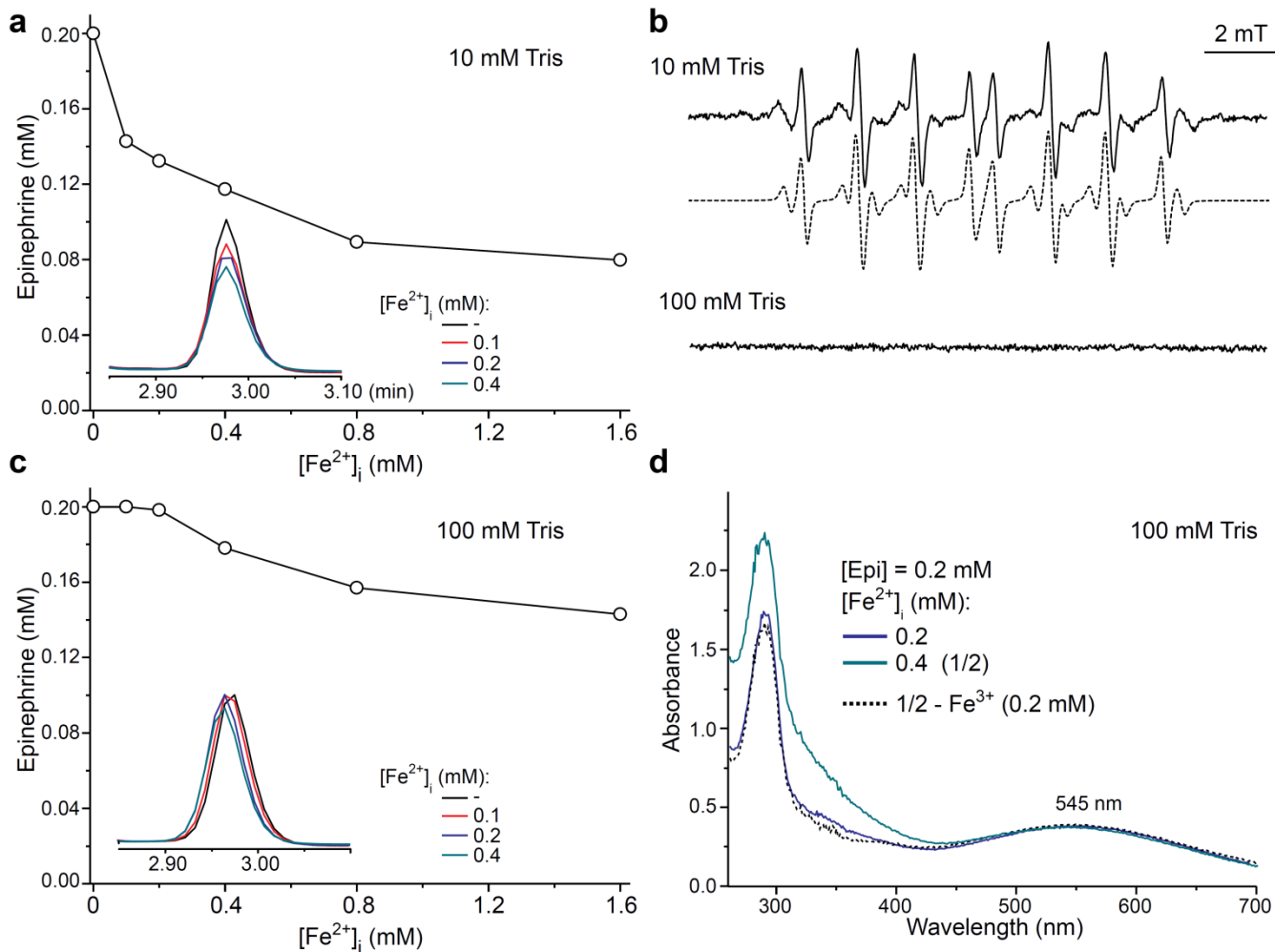


Figure S5 Antioxidative performance of 10 mM and 100 mM Tris, pH 7.4. (a) The concentration of Epi following 5 min incubation with different [Fe²⁺]_i in 10 mM Tris buffer. Inset: Epi peaks in HPLC chromatograms. (b) EPR spectra of adducts of DEPMPO spin trap (5 mM), illustrating the capacity of Tris to remove hydroxyl radical (HO[•] is produced in the Fenton reaction: Fe²⁺ (0.4 mM) + H₂O₂ (1.2 mM)). Spectrum in 10 mM Tris is composed of DEPMPO adducts with HO[•] (65%) and Tris-derived C-centred radical (35%), as determined by spectral simulation (dashed line). No EPR signal could be observed in 100 mM Tris. (c) The concentration of Epi following 5 min incubation with different [Fe²⁺]_i in 100 mM Tris buffer. Inset: Epi peaks in HPLC chromatograms. (d) UV-Vis spectra of Epi/Fe²⁺ systems after 5 min incubation in 100 mM Tris. No further changes were observed. Dashed line represents the subtraction of experimental spectra. The resulting spectrum with λ_{max} = 545 nm in the system with [Epi]/[Fe²⁺]_i = 0.5, represents the sum of the spectrum for [Epi]/[Fe²⁺]_i = 1 and the spectrum of [Fe³⁺] = 0.2 mM.

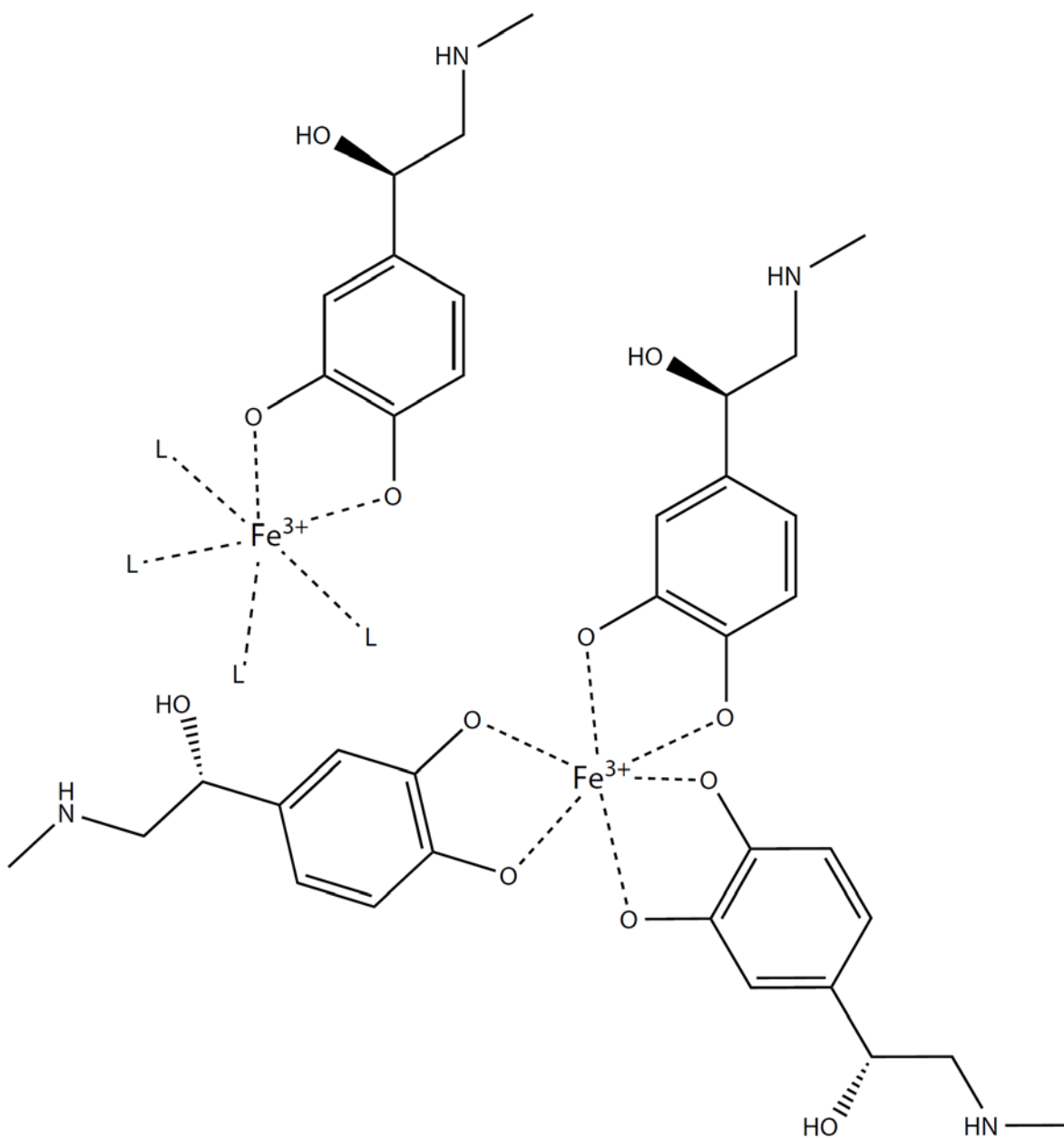


Figure S6 Schematic presentation of the chemical structures of Epi-Fe³⁺ complexes. L – other ligands (e.g. OH⁻, HPO₄²⁻, H₂PO₄⁻, H₂O).

Table S1 Reactions that are relevant for Fe²⁺ oxidation at pH 7.4.

No	Reaction	k (M ⁻¹ s ⁻¹)	Ref
1	$\text{Fe}^{2+} + \text{O}_2 \rightarrow \text{Fe}^{3+} + \text{O}_2^{\bullet-}$	4×10^{-2}	(a)
2	$\text{Fe}^{2+} + \text{O}_2^{\bullet-} + 2\text{H}^+ \rightarrow \text{Fe}^{3+} + \text{H}_2\text{O}_2$	1×10^7	(b)
3	$\text{Fe}^{3+} + \text{O}_2^{\bullet-} \rightarrow \text{Fe}^{2+} + \text{O}_2$	1.5×10^8	
4 [*]	$\text{Fe}^{2+} + \text{H}_2\text{O}_2 \rightarrow \text{Fe}^{3+} + \text{HO}^{\bullet} + \text{OH}^-$	10^2	
5	$\text{Fe}^{2+} + \text{HO}^{\bullet} \rightarrow \text{FeOH}^{2+}$	3.2×10^8	
6 ^{**}	$2\text{H}_2\text{O}_2 \text{ (CAT)} \rightarrow 2\text{H}_2\text{O} + \text{O}_2$		

^{*} Fenton reaction; ^{**}The mechanism of catalase-mediated degradation of H₂O₂. The concentration of accumulated H₂O₂ is calculated as 2×Δ[O₂] that is induced by CAT.

(a) King, D. W.; Lounsbury, H. A.; Millero, F. J. *Environ. Sci. Technol.*, 1995, **29**, 818-825.

(b) Halliwell, B. & Gutteridge, J. M. C. *Free Radicals in Biology and Medicine*, 4th ed, Clarendon Press, Oxford, 2007.